NIH Public Access
Author Manuscript
Neurosurgery. Author manuscript; available in PMC 2010 May 1.

Published in final edited form as:
Neurosurgery. 2009 May ; 64(5): 965–972. doi:10.1227/01.NEU.0000344150.81021.AA.

In Vitro Characterization of a Targeted, Dye-Loaded Nanodevice for Intraoperative Tumor Delineation

Daniel A. Orringer, M.D.[1], **Yong-Eun L. Koo, Ph.D.**[2], **Thomas Chen**[4], **Gwangseong Kim, Ph.D.**[2], **Hoe Jin Hah, Ph.D.**[2], **Hao Xu, Ph.D.**[3], **Shouyan Wang, Ph.D.**[2], **Richard Keep, Ph.D.**[1], **Martin A. Philbert, Ph.D.**[3], **Raoul Kopelman, Ph.D.**[2], and **Oren Sagher, M.D.**[1]

1 *Department of Neurosurgery, University of Michigan Health System, Ann Arbor, Michigan*

2 *Department of Chemistry, University of Michigan, Ann Arbor, Michigan*

3 *Department of Toxicology, University of Michigan, Ann Arbor, Michigan*

4 *University of Michigan, Ann Arbor, Michigan*

Abstract

OBJECTIVE—To synthesize and complete *in vitro* characterization of a novel, tumor-targeted nanodevice for visible intraoperative delineation of brain tumors.

METHODS—The ability of dye-loaded polyacrylamide nanoparticles (NPs) containing methylene blue, Coomassie blue, or indocyanine green, to cause color change in the 9L glioma cell lines was evaluated. Cells were incubated with dye-loaded NPs, photographed, and analyzed colorimetrically. Confocal microscopy was used to determine subcellular localization of NPs in treated cells.

RESULTS—Incubation of glioma cell lines with dye-loaded NPs resulted in clearly visible, quantifiable cell tagging in a dose- and time-dependent fashion. Dye-loaded NPs were observed to bind to the surface and become internalized by glioma cells. Coating the NP surface with F3, a peptide that binds to the tumor cell surface receptor nucleolin, significantly increased NP affinity for glioma cells. F3-targeting also significantly increased the rate of cell tagging by dye-loaded NPs. Finally, F3-targeted NPs demonstrated specificity for targeting various cancer cell lines based on their surface expression of cell surface nucleolin.

CONCLUSIONS—F3-targeted dye-loaded NPs efficiently cause definitive color change in glioma cells. This report represents the first use of targeted NPs to cause a visible color change in tumor cell lines. Similar nanodevices may be used in the future to enable visible intraoperative tumor delineation during tumor resection.

Keywords

Nanoparticle; Brain tumor; Tumor imaging

INTRODUCTION

Patient survival for both pediatric and adult brain tumors is maximized by radiographically complete surgical resection (16). However, even with the best microsurgical resection, residual magnetic resonance imaging (MRI)-demonstrable tumor may be left behind. Advances in

CORRESPONDENCE: Oren Sagher, M.D., Department of Neurosurgery, University of Michigan Health System, 1500 E. Medical Center Drive, Room 3552 Taubman Center, Ann Arbor, MI 48109-5338, Phone: 734-936-9593; Fax: 734-936-9294, E-mail: E-mail: osagher@umich.edu.

NIH-PA Author Manuscript
NIH-PA Author Manuscript
NIH-PA Author Manuscript

NIH-PA Author Manuscript

NIH-PA Author Manuscript

NIH-PA Author Manuscript

nanotechnology may ultimately enable a more complete resection of brain tumors and lead to novel adjuvant therapies to address residual or occult tumor at the time of surgery(9).

A variety of techniques and devices have been developed to enable radiographically complete resection, including frameless stereotaxy and intraoperative MRI. While the implementation of these techniques has expanded, their ability to improve surgical and patient outcome remains unproven (12,24). Since 1947, investigators have proposed the use of multiple candidate compounds to aid in the recognition of neoplastic tissue during resection (1,4,11,13,18,20). However, due to lack of adequate visible contrast at tumor margins, dye toxicity, and/or the need for specialized optical imaging equipment, these dyes have yet to gain widespread clinical use.

Nanoparticles (NPs) can be engineered to deliver a variety of small molecules such as MRI contrast agents and chemotherapy to brain tumors. NPs tend to accumulate in brain tumors by passing through areas of blood-brain barrier breakdown and are likely retained in brain tumors through the enhanced permeability and retention effect (10). Furthermore, NPs can be targeted directly to neoplastic cells through tumor-specific ligands. Among the ligands used for targeting NPs to tumors are chlorotoxin (7) and F3 (15), peptides that bind to specific receptors expressed on brain tumor cells. Chlorotoxin targets glioma cells by binding to cell surface chloride channels. F3, a 31-amino acid peptide that binds to nucleolin, a cell surface receptor, has the added benefit of binding to angiogenic vasculature in addition to tumor cells (2).

We have recently shown that F3-targeted polyacrylamide NPs can efficiently deliver diagnostic and therapeutic small molecules to implanted 9L gliomas in rats. These nanoparticles localize to implanted gliomas within minutes and persist for over 2 hours after a single intravenous dose (15). Polyacrylamide nanoplatforms can be loaded with a wide variety of small molecules, including visible dyes. Here, we report the synthesis and *in vitro* characterization of a polyacrylamide NP loaded with visible dye and coated with F3-targeting peptide to enable specific delivery to tumor cells. Ultimately, this novel nanodevice may be capable of improving the ability of neurosurgeons to achieve radiographically complete resection of brain tumors by visibly delineating tumor margins without the need of any specialized imaging equipment.

MATERIALS AND METHODS

Fluorescent F3 peptide was prepared as follows: HiLyte Fluor™ 647 C2 maleimide (0.90×10^{-3} mmol; Anaspec, San Jose, CA) was dissolved in 1 mL phosphate-buffered saline (PBS) (pH 7.2) and mixed with 0.2 mL of 4.5 mM of F3-Cys peptide solution (KDEPQRRSARLSAKPAPPKPEPKPKKAPAKKC; PolyPeptide Laboratories, Inc., Torrance, CA) in PBS was added to the HiLyte solution. The mixture solution was stirred overnight at 37°C. L-Cysteine (0.1 mmol) was excessively added to the mixture under stirring and reacted for 1 h at 37°C to block the reactive site of unreacted HiLyte.

Nanoparticle synthesis

Synthesis of Coomassie blue or indocyanine green-loaded polyacrylamide (PAA) NPs—Amine-functionalized PAA NPs were synthesized by a microemulsion method. Briefly, an aqueous solution containing acrylamide (8.58 mmol; Sigma-Aldrich Co., St. Louis, MO), N-(3-Aminopropyl)methacrylamide hydrochloride salt (0.25 mmol; Polysciences, Inc., Warrington, PA) and methylene-bis-acrylamide (1.20 mmol; Sigma-Aldrich Co.) is mixed with hexane solution (36 mL; Sigma-Aldrich Co.) containing Brij 30 (6.85 mmol; Sigma-Aldrich Co.) and dioctyl sulfosuccinate (AOT) (2.88 mmol; Sigma-Aldrich Co.). NP synthesis was initiated by ammoninum persulfate (2.8×10^{-5} mmol; Sigma-Aldrich Co.) and N,N,N′,N′-tetramethyl ethylenediamine (TEMED) (0.54 mmol; Sigma-Aldrich Co.). In the case of methylene blue-loaded particles, methylene blue succinimidyl ester (4.64 μmol; Biotech

NIH-PA Author Manuscript

NIH-PA Author Manuscript

NIH-PA Author Manuscript

GmbH, Berlin, Germany) was added to the aqueous monomer solution and reacted under the same conditions. After overnight reaction at room temperature, the NP solution was evaporated and the resultant thick residue was dispersed in ethanol (95%; Decon Labs, Inc., King of Prussia, PA). Thorough washing with ethanol and water followed by freeze-drying produced a fine powder of NPs. Coomassie blue (Brilliant Blue G; Sigma-Aldrich Co.) or indocyanine green (Cardiogreen; Sigma-Aldrich Co.) was post-loaded into blank particles at room temperature by adding dyes, dissolved in DMSO into the NP suspension in PBS, stirring the mixture for 2 h and washing multiple times with water and PBS multiple times.

Synthesis of peptide-targeted dye-loaded PAA NPs—Peptide conjugation to surface amines of the NP surface was made through a bifunctional conjugating ligand, Sulfo-SMCC (Thermo Fisher Scientific, Inc., Rockford, IL). The NP suspension of 20 mg/mL in PBS (pH 7.4) was mixed with Sulfo-SMCC and stirred at room temperature for 2 h and then subjected to thorough washing to remove any unreacted ligands. The collected NP solution was treated with 2×10^{-3} mmol of wild-type F3-Cys, scrambled F3-Cys (PKAARALPSQRSRPPEKAKKPPDKPAPEKKKC; SynBioSci Corp., Livermore, CA) or HIV TAT-cysteine (SynBioSci Corp.) and gently stirred overnight at room temperature. The reaction mixture was then treated with L-Cysteine (1.43×10^{-2} mmol) for 2 h in order to scavenge any unreacted ligand and to minimize the potential for non-specific binding. The resultant NP solution was thoroughly washed with water and PBS. The absorbance of the NP solutions was measured to evaluate dye content.

Scanning electron microscopy (SEM)

The NP solution of 0.2 mg/mL was prepared in water and a drop of the NP solution was placed on the SEM specimen mount (aluminum) and dried gradually at room temperature. The sample was then sputter-coated with gold and the SEM images were taken using a Phillips XL30 scanning electron microscope.

Cell culture

The MDA-MB-435 human melanoma cell line was cultured in Dulbecco modified Eagle medium with 10% fetal bovine serum (FBS), 1% NaPyruvate, and 1% non-essential amino acids. The MCF-7 human breast cancer cell line and 9L gliosarcoma cells were cultured in RPMI 1640 medium (Invitrogen, Carlsbad, CA) with 10% FBS. For fluorescent imaging on a confocal microscope, cells were cultivated on the cover slips.

Fluorescent F3 peptide assay

Three different cell lines (MDA-MB-435, MCF-7, and 9L) were incubated with 39.8 uM of Hilyte-647 fluorophore labeled F3 peptide for 2 h at 37°C and washed 3 times with cell media to remove unbound peptides. Confocal images were obtained using a 647-nm excitation light source and a band-pass filter transparent between 675–725 nm on an Olympus IX70 confocal microscope connected to an UltraVIEW confocal laser scanning microscope (Life Science Resources, Cambridge, UK) equipped with an Ar-Kr laser (Omnichrome Series 43; Melles Griot, Carlsbad, CA). The cell targeting efficiency of the F3 peptide was quantified by analyzing pixel intensity per cells on confocal images.

Nanoparticle treatment and cell tagging assay by visual colorimetry

Each of the cell lines was harvested from culture, washed with PBS, and counted. Cells (3×10^{6}) were aliquoted into microcentrifuge tubes and incubated with dye-loaded NPs for 2 h at 37°C in a rotating incubator. The samples were then washed with PBS to remove free NPs. Cells were centrifuged in an Eppendorf microcentrifuge at 6000 rpm for 3 min. Cell pellets were photographed on white backgrounds using a LX-100 CCD video microscope (Caltex

NIH-PA Author Manuscript

NIH-PA Author Manuscript

NIH-PA Author Manuscript

Scientific, Irvine, CA). Each experiment was carried out 3 times and each data point represents an average value of 3 independent samples.

Subcellular location study by confocal microscopy

Each cell line was treated with 0.25 mg/mL F3-targeted methylene blue and Coomassie blue (CB)-loaded PAA NPs. After 1 h incubation, unbound NPs were washed away by changing the cell culture media 3 times. Distribution of F3-targeted NPs in or on the cells was imaged and analyzed by confocal microscopy as described for the fluorescent peptide assay.

Quantitative evaluation of staining

Images acquired as described above processes were imported into Image J software (public domain; National Institutes of Health, Bethesda, MD). A region of interest (ROI) was created consisting of approximately 2000 pixels in the center of the cell pellet. The RGB histogram plug-in was used to estimate the mean red, green, and blue components of the color in the ROI. Adobe Photoshop software (San Jose, CA) was used to calculate corresponding hue, saturation, and brightness of the ROI. Because measured saturation correlates with the perceived depth of color change, it was used to judge the extent of cell tagging.

Statistical analysis

Data sets were evaluated using the Microsoft Excel data analysis statistics package (Microsoft Corp., Redmond, CA) to run unpaired, 2-tailed *t*-tests, with statistical significance set at $P = 0.05$.

RESULTS

Nanoparticle characterization

NPs were soluble in cell culture media at 5 mg/mL. NP size was confirmed to be approximately 30 nm by scanning electron microscopy (Fig. 1). The estimated molecular weight of the NPs was 0.8 million Da. Qualitatively, the solutions appeared deep blue. Quantitatively, based on absorbance data, the Coomassie blue content of the NP solutions was determined to be 3.4% w/w (data not shown). The content of methylene blue NPs was 0.01%. The dye content of indocyanine green NPs was 5%. Photostability of all 3 dyes in the NPs was similar to that of the free dye (98%), and dye-leaching was negligible in PBS.

Visible glioma cell tagging

To assess the ability of the dye-loaded NPs to visibly stain tumor cells, we carried out a series of experiments using the 9L gliosarcoma cell line, in which cells were incubated with CB-loaded, methylene blue-loaded, or indocyanine green-loaded polyacrylamide NPs. Qualitatively, each of the NPs produced a clearly visible color change in 9L gliosarcoma cells (Fig. 2). The observed color change was visible under normal lighting conditions. The color of cell pellets was qualitatively judged by 2 neurosurgeons (Drs. Oren Sagher and Karin Muraszko) to be adequately distinct from the visual appearance of normal brain tissue typically found surrounding a brain tumor.

Because the depth of color change in glioma cells was greatest with CB-loaded NPs, the remaining experiments were carried out with CB-loaded NPs. By quantitative evaluation of the color saturation within each cell pellet, differences in the depth of staining were calculated. Measured saturation values were found to correlate with depth of color change in treated glioma cells. The threshold for visible color change was a saturation value of approximately 30.

NIH-PA Author Manuscript

NIH-PA Author Manuscript

NIH-PA Author Manuscript

Subcellular nanoparticle localization

CB-loaded NPs were co-loaded with methylene blue, which can be used as a fluorescent marker in darkfield confocal microscopy. Co-loaded NPs were used to evaluate whether NPs were internalized or remained bound to the cell surface. NP concentration of 0.25 mg/mL and a 15-min incubation time were chosen to minimize non-specific binding. F3-targeted NPs appeared to be concentrated within the cytoplasm of the NPs within vesicles and, to a lesser extent, NPs were observed coating the cell surface (Fig. 2E). Non-targeted NPs were not taken-up by cells in sufficient quantity to cause visible fluorescence (data not shown).

Kinetics of glioma cell color change

Cell pellet saturation increased in a sigmoidal fashion with increasing NP concentration (Fig 3). The estimated NP concentration required to achieve visible color change in cell pellets was 0.11 mg NP/mL for F3-targeted CB-loaded NPs and 0.31 mg NP/mL for non-targeted CB-loaded NPs. With the exception of a concentration of 0.0156 mg NP/mL, F3-targeted NPs caused a statistically significant increase in cell tagging ($P < 0.01$) at all NP doses tested. The greatest difference in color change caused by F3-targeted, compared to non-targeted NPs, occurred at a NP concentration of 0.125 mg/mL, where color change was 5-fold greater in cells treated with F3-targeted NPs. The increase in color change was minimal beyond a concentration of 0.25 mg/mL for F3-targeted CB-loaded NPs compared with 0.5 mg NP/mL for non-targeted CB-loaded NPs.

Cell pellet saturation increased in a logarithmic pattern with increased incubation time (Fig. 4). The estimated incubation time required to achieve visible color change in cell pellets treated with 0.0625 mg/mL NP was 10 min for F3-targeted CB-loaded NPs and 27 min for non-targeted CB-loaded NPs. At each time point, F3-targeted NPs caused a statistically significant increase in cell tagging ($P < 0.04$). The greatest difference in color change by non-targeted compared to F3-targeted NPs occurred after 1 min, when color change was 3.3-fold greater in cells treated with F3-targeted NPs. An increase in color change was minimal beyond a concentration of 3 h for both F3-targeted and non-targeted CB-loaded NPs.

Specificity of F3-targeted nanoparticles for nucleolin-expressing cell lines

F3 binds to angiogenic vasculature and tumor cells by binding to nucleolin expressed on the cell surface (1). The MDA-MB-435 breast cell line is known to express high levels of nucleolin (4), while the MCF-7 breast cancer cell line expresses low levels of nucleolin (Table 1). Like the MDA-MB-435 cell line, the 9L cell line expresses high levels of nucleolin. There was a significant ($P < 0.005$) increase in cell color change by F3-targeted NPs compared to non-targeted NPs in the MDA-MB-435, MCF-7, and 9L cell lines (Fig. 5). However, the relative magnitude of the increase in color change by F3-targeted NPs in MCF-7 cells was significantly less than the increase in color change in the MDA-MB-435 and 9L cells. The magnitude of increase in the color change for TAT-targeted NP, which enters the cell via a receptor-independent mechanism (6), was statistically identical for MCF-7, MDA-MB-435, and 9L cells (data not shown).

Confirmation of F3 targeting

Finally, we aimed to confirm that targeting of NPs to nucleolin-expressing cells is indeed dependent on F3-nucleolin interactions. We compared the 9L cell color change caused by NPs targeted with wild-type F3 to the color change caused by NPs targeted with scrambled F3. While the incubation of 9L cells with wild-type F3-targeted NPs at a concentration of 0.0625 mg NP/mL caused a 3.1-fold increase in cell tagging compared to non-targeted NP; scrambled F3-targeted NPs caused no significant increase in cell tagging (Fig. 6).

NIH-PA Author Manuscript

NIH-PA Author Manuscript

NIH-PA Author Manuscript

DISCUSSION

By improving the efficacy of perioperative imaging and therapy, nanotechnology may revolutionize the management of brain tumors. For example, NPs may be developed to visibly delineate brain tumors to enable more accurate and complete resection. This study represents the first published evidence that dye-loaded NPs can cause color change, visible to the naked eye, in glioma cells.

Of the candidate dyes we examined, CB appears to be the most favorable for creating a dye-loaded NP for brain tumor delineation. CB-loaded NPs can be easily synthesized by post-loading coomassie blue into poly-acrylamide NPs and provide the best visual contrast characteristics among the 3 dye-loaded NPs tested. Although the safety of using CB within the nervous system is unknown, it has little systemic toxicity in humans, even when administered intravenously at very high doses (21).

After demonstrating qualitative cell tagging, we studied the mechanism of NP-cell interactions. Visual tagging of glioma cells by dye-loaded NPs appears to occur as a result of cell surface binding and internalization of NPs into the cytoplasm. F3-targeted NPs bind to glioma cells and are more readily internalized than non-targeted NPs. These data are consistent with previous evaluations of targeted NP uptake by tumor cells *in vitro* (23). We also note that cellular internalization of the nanoparticles synthesized here would be predicted based on their size (5).

In addition to demonstrating a qualitative color change in glioma cells, we sought to develop a quantitative method for measuring the depth of color change. Measurements of hue, saturation, and brightness have been previously employed to quantify color in other applications (3). We measured the hue, saturation, and brightness of treated cells to quantitatively judge NP-induced color change. We believe the saturation scale we report here is valid, since increasing saturation values correlate well with the depth of blue color perceived by the human eye. Saturation quantification enabled us to explore subtle differences in color change under different experimental conditions.

The saturation scale was used to analyze both dose and time response curves for NP-treated cells. Color change in NP-treated cells increased in a sigmoidal fashion with increasing NP concentration for both F3-targeted and non-targeted NPs. The addition of F3-targeting peptide to the surface of the NPs resulted in a significant decrease in the dose of NPs necessary to cause visible color change. Since key biophysical properties including size, absorbance, solubility, and concentration are identical for targeted and non-targeted NPs, we attribute the differences in the dose of NP and treatment duration required to cause color change to an increased affinity of the F3-targeted NPs for glioma cells. We do however acknowledge that significant non-specific binding was observed, suggesting that factors other than F3-nucleolin interactions may play a role in nanoparticle internalization.

Nonetheless, to verify that the increased affinity of F3-targeted NPs, compared to non-targeted NPs, for glioma cells is indeed due to specific cell surface receptor interactions, we created a peptide with the same amino acid composition in a scrambled sequence that has been previously shown to be ineffective in binding nucleolin (14). The observation that wild-type, but not scrambled-F3-targeted NPs, induced color change in glioma cells suggests that a specific primary, secondary and/or tertiary structure of F3 peptide is necessary for interactions with nucleolin receptors on glioma cells that enable NP uptake. Therefore, we believe that the enhanced uptake of F3-targeted NPs by glioma cells is mediated through specific F3-nucleolin interactions.

NIH-PA Author Manuscript

NIH-PA Author Manuscript

NIH-PA Author Manuscript

While it would be ideal to compare F3-targeted NP uptake in nucleolin-expressing cell lines (eg, 9L, MDA-MB-435) to uptake in a cell line lacking nucleolin altogether, we are unaware of such a cell line and, to our knowledge, creating a genetic knockout for nucleolin is lethal (Rehemtulla, personal communication). However, we were able to compare F3-targeted NP uptake by a cell line expressing high levels of nucleolin (9L and MDA-MB-435) to uptake by cell lines expressing low levels of nucleolin (MCF-7). While there was a significant increase in F3-targeted NP uptake by MCF-7 cells, the magnitude of the increase was much greater in cells expressing high levels of nucleolin. Importantly, all cell lines tested demonstrated a statistically identical increase in color change when treated with HIV TAT peptide-targeted NPs, which enter cells in a receptor independent mechanism. From these experiments, we infer that F3-nucleolin interactions are indeed responsible for the enhanced uptake of F3-targeted NPs. Similar experiments utilizing human brain tumor cell lines and primary brain tumor cultures will be required to evaluate whether F3 is an efficient targeting option for nanoparticles designed for use in brain tumor patients. These experiments do however suggest that NPs can be selectively targeted to specific cancer cell populations based on the expression of cell surface molecules.

Implanted rat gliomas have been efficiently targeted with intravenous administration of F3-targeted NPs (15). Chlorotoxin, a peptide with a high affinity for chloride channels and which is upregulated in glioma cells, has also been proposed as a means for NP targeting of implanted gliomas (7,23). It remains unclear whether F3 or chlorotoxin will have relevance in targeting human brain tumors. However, due to the chemical flexibility of the polyacrylamide nanoplatform we have characterized here, it would be reasonable to attach almost any peptide or small molecule with a high affinity and specificity for glioma cells to its surface. Furthermore, it is reasonable to infer that NPs could ultimately be tailored for an individual tumor based on its receptor expression profile.

Based on the data presented here, further studies are necessary to evaluate whether the NP-induced color change in glioma cells observed *in vitro* will translate into color change in gliomas *in vivo*. Several investigators have previously demonstrated impressive *in vivo* delineation of implanted brain tumors using the visible dyes bromophenol blue (13) and indocyanine green (1). Selective dye uptake by tumors is thought to occur because certain compounds such as bromophenol blue and indocyanine green cross the blood-tumor barrier more readily than the blood-brain barrier. Due to the lack of data in brain tumor patients, it is unclear whether bromophenol blue and indocyanine green would be applicable to delineating gliomas. However, based on studies of fluorescent dyes such as fluorescein (18) and 5-ALA (19), that diffuse through the blood-brain barrier, it is likely that there will be regions containing tumor cells that have not been stained by dye.

In addition to a non-homogenous distribution within the tumor, toxicity may be a possible limitation of the success of visible dyes for tumor delineation. The toxicity of bromophenol blue in humans is unknown. Moreover, at doses necessary for tumor delineation, profound dye uptake by all tissues (with the exception of the brain) is observed when free dye is injected in rat glioma models (Orringer DA, unpublished data). The lowest necessary dose of indocyanine green required to cause visible color change in implanted gliomas, even when coadministered with the tumor-specific blood-brain barrier relaxant RMP-7, is 4.5 to 6 times the upper limit currently approved by the Food and Drug Administration for use in humans (1). By facilitating the delivery of dye specifically to the tumor, a targeted nanodevice would likely decrease the dose of systemically administered dye needed for visible delineation.

A Cy5.5-chlorotoxin bioconjugate reported to accurately delineate implanted 9L glioma margins (22) is currently in human trials and holds promise for delineating tumors at a non-toxic level, since and it specifically targets glioma cells. In addition, chlorotoxin-targeted

NIH-PA Author Manuscript

NIH-PA Author Manuscript

NIH-PA Author Manuscript

Cy5.5-loaded NPs have been shown to enter 9L glioma cells *in vitro* (23) and delineate implanted 9L gliomas (7). While chlorotoxin-targeted compounds hold promise with respect to delineating tumor margins with greater specificity than free dyes, a significant barrier to the implementation of Cy5.5-based compounds to tumor resection relates to the imaging conditions necessary for visualization. First, sophisticated fluorescent or bioluminescence imaging technology is necessary to visualize Cy5.5 stained tissue. Furthermore, conventional microsurgical dissection would be difficult under the darkened lighting conditions necessary to visualize the fluorescent Cy5.5. Working in a well-lit operative field is essential when trying to minimize collateral damage to adjacent eloquent cortex and supporting vasculature during a tumor resection. Therefore, the ideal optical contrast agent would be a dye that could be easily visualized under traditional lighting conditions currently used for tumor resection.

The nanodevice reported here has been designed to overcome the limitations of previously reported compounds for visible tumor delineation. Like chlorotoxin-targeted NPs (7,23), the F3-targeted NPs target glioma cells and implanted gliomas through both passive and active mechanisms, and therefore should be able to efficiently deliver dye to tumors *in vivo* at non-toxic doses. Furthermore, in contrast to Cy5.5-based compounds, we predict that intravenously administered, CB-loaded NPs will provide excellent optical contrast, visible to the naked eye, between tumor and normal brain in the setting of glioma resection.

Given the relative scarcity of data on dye-loaded nanoparticles in tumor models, research utilizing tumor models will be required to determine whether nanoparticle-induced color change in tumor tissue will occur *in vivo* to the extent we have observed *in vitro*. Among the variables currently under investigation are nanoparticle dye content required for visible color change, the extent of dye leaching from nanoparticles in circulation, the role of targeting peptides in tumor cell uptake, the role of blood brain barrier breakdown on nanoparticle extravasation, the kinetic parameters required to optimize visible tumor delineation and histologic accuracy of color change at the tumor-brain interface. In addition, although we have previously demonstrated the non-toxicity of polyacrylamide nanoparticles in rats (8,17), further work in animal tumor models will be required to ensure that dye-loaded nanoparticles do not have significant systemic toxicity or toxicity to specific populations of cells inside or outside of the nervous system. *In vivo* studies in tumor models will guide further modification of nanoparticles required to create clinically useful tumor-targeted dye-loaded NPs.

CONCLUSIONS

F3-targeted, CB-loaded NPs visibly tag glioma cell lines *in vitro*. The color change in glioma cells induced by NP treatment is readily visible to the naked eye. The ability of NPs to cause color change in glioma cells is facilitated by coating their surface with F3 peptides. Peptide-targeted NPs are capable of selectively binding to specific cell populations via cell surface receptors. Ultimately, *in vivo* testing in relevant brain tumor models will be required to determine the clinical significance of the novel visible contrast effects of targeted, dye-loaded NPs described here.

Acknowledgments

This work was supported by grants from the National Institute of Biomedical Imaging and Bioengineering (1R01EB007977-01, RK), the National Cancer Institute (1R21CA125297-01A1, RK and 1F32CA126295-01A1, DO) and the Congress of Neurologic Surgeons Basic/Translational Resident Research Fellowship (DO). The authors thank Holly Wagner for her generous assistance in editing this manuscript.

NIH-PA Author Manuscript

NIH-PA Author Manuscript

NIH-PA Author Manuscript

References

1. Britz G, Ghatan S, Spence AM, Berger MS. Intracarotid RMP-7 enhanced indocyanine green staining of tumors in a rat glioma model. Journal of Neurooncology 2002;56:227–232.
2. Christian S, Pilch J, Akerman ME, Porkka K, Laakkonen P, Ruoslahti E. Nucleolin expressed at the cell surface is a marker of endothelial cells in angiogenic blood vessels. Journal of Cell Biology 2003;163:871–878. [PubMed: 14638862]
3. Fan, S.; Dyer, CR.; Hubbard, L. Quantification and correction of iris color: Technical Report 1495. University of Wisconsin-Madison; 2003.
4. Hansen D, Spence AM, Carski T, Berger M. Indocyanine green (ICG) staining and demarcation of tumor margins in a rat glioma model. Surgical Neurology 1993;40:451–456. [PubMed: 7694381]
5. Jiang W, Kim BY, Rutka JT, Chan WC. Nanoparticle-mediated cellular response is size-dependent. Nat Nanotechnol 2008;3:145–150. [PubMed: 18654486]
6. Josephson L, Tung CH, Moore A, Weissleder R. High-efficiency intracellular magnetic labeling with novel superparamagnetic-Tat peptide conjugates. Bioconjugate Chemistry 1999;10:186–191. [PubMed: 10077466]
7. Kircher M, Mahmood U, King RS, Weissleder R, Josephson L. A multimodal nanoparticle for preoperative magnetic resonance imaging and intraoperative optical brain tumor delineation. Cancer Research 2003;63
8. Koo YE, Reddy GR, Bhojani M, Schneider R, Philbert MA, Rehemtulla A, Ross BD, Kopelman R. Brain Cancer Diagnosis and Therapy with Nano-Platforms. Advanced Drug Delivery Reviews 2006;58:1556–1577. [PubMed: 17107738]
9. Leary S, Liu CY, Yu C, Apuzzo ML. Toward the emergence of nanoneurosurgery: part I--progress in nanoscience, nanotechnology, and the comprehension of events in the mesoscale realm. Neurosurgery 2005;57:606–634. [PubMed: 16239874]
10. Maeda H, Wu J, Sawa T, Matsumura Y, Hori K. Tumor vascular permeability and the EPR effect in macromolecular therapeutics: a review. Journal of Controlled Release 2000;65:271–284. [PubMed: 10699287]
11. Moore G. Fluorescein as an agent in the differentiation of normal and malignant tissues. Science 1947;106:130–131. [PubMed: 17750790]
12. Muragaki Y, Iseki H, Maruyama T, Kawamata T, Yamane F, Nakamura R, Kubo O, Takakura K, Hori T. Usefulness of intraoperative magnetic resonance imaging for glioma surgery. Acta Neurochir 2006;(Suppl):67–75.
13. Ozawa T, Britz GW, Kinder DH, Spence AM, VandenBerg S, Lamborn KR, Deen DF, Berger MS. Bromophenol blue staining of tumors in a rat glioma model. Neurosurgery 2005;57:1041–1047. [PubMed: 16284574]
14. Porkka K, Laakkonen P, Hoffman JA, Bernasconi M, Ruoslahti E. A fragment of the HMGN2 protein homes to the nuclei of tumor cells and tumor endothelial cells in vivo. Proc Natl Acad Sci U S A 2002;99:7444–7449. [PubMed: 12032302]
15. Reddy GR, Bhojani MS, McConville P, Moody J, Moffat BA, Hall DE, Kim G, Koo YE, Woolliscroft MJ, Sugai JV, Johnson TD, Philbert MA, Kopelman R, Rehemtulla A, Ross BD. Vascular targeted nanoparticles for imaging and treatment of brain tumors. Clin Cancer Res 2006;12:6677–6686. [PubMed: 17121886]
16. Sanai N, Berger MS. Glioma extent of resection and its impact on patient outcome. Neurosurgery 2008;62:753–764. [PubMed: 18496181]discussion 264–756
17. Schneider, R. Toxicology. Ann Arbor: University of Michigan; 2005. Characterization of polyacrylamide nanoparticles for biomedical applications: toxicology, pharmacology, and therapy.
18. Shinoda J, Yano H, Yoshimura S, Okumura A, Kaku Y, Iwama T, Sakai N. Fluorescence-guided resection of glioblastoma multiforme by using high-dose fluorescein sodium. Technical note. J Neurosurg 2003;99:597–603. [PubMed: 12959452]
19. Stummer W, Novotny A, Stepp H, Goetz C, Bise K, Reulen HJ. Fluorescence-guided resection of glioblastoma multiforme by using 5-aminolevulinic acid-induced porphyrins: a prospective study in 52 consecutive patients. J Neurosurg 2000;93:1003–1013. [PubMed: 11117842]

NIH-PA Author Manuscript

NIH-PA Author Manuscript

NIH-PA Author Manuscript

20. Stummer W, Pichlmeier U, Meinel T, Wiestler OD, Zanella F, Reulen HJ. Fluorescence-guided surgery with 5-aminolevulinic acid for resection of malignant glioma: a randomised controlled multicentre phase III trial. Lancet Oncol 2006;7:392–401. [PubMed: 16648043]

21. Taylor SH, Shillingford JP. Clinical Applications of Coomassie Blue. Br Heart J 1959;21:497–504. [PubMed: 18610134]

22. Veiseh M, Gabikian P, Bahrami SB, Veiseh O, Zhang M, Hackman RC, Ravanpay AC, Stroud MR, Kusuma Y, Hansen SJ, Kwok D, Munoz NM, Sze RW, Grady WM, Greenberg NM, Ellenbogen RG, Olson JM. Tumor paint: a chlorotoxin:Cy5.5 bioconjugate for intraoperative visualization of cancer foci. Cancer Res 2007;67:6882–6888. [PubMed: 17638899]

23. Veiseh O, Sun C, Gunn J, Kohler N, Gabikian P, Lee D, Bhattarai N, Ellenbogen R, Sze R, Hallahan A, Olson J, Zhang M. Optical and MRI multifunctional nanoprobe for targeting gliomas. Nano Lett 2005;5:1003–1008. [PubMed: 15943433]

24. Willems PW, Taphoorn MJ, Burger H, Berkelbach van der Sprenkel JW, Tulleken CA. Effectiveness of neuronavigation in resecting solitary intracerebral contrast-enhancing tumors: a randomized controlled trial. J Neurosurg 2006;104:360–368. [PubMed: 16572647]

NIH-PA Author Manuscript
NIH-PA Author Manuscript
NIH-PA Author Manuscript

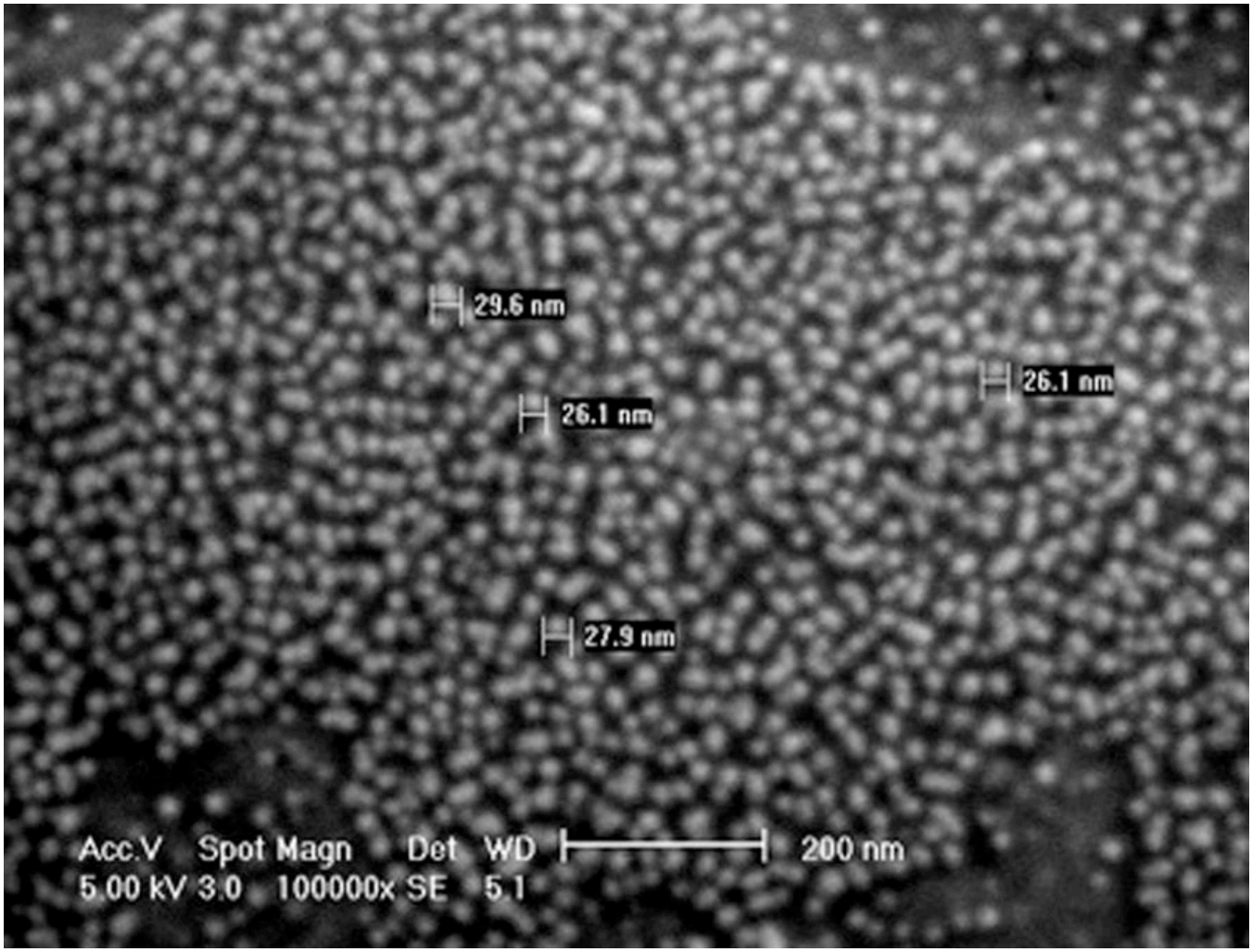

Figure 1.
Scanning electron micrograph of F3-targeted, CB-loaded NPs.

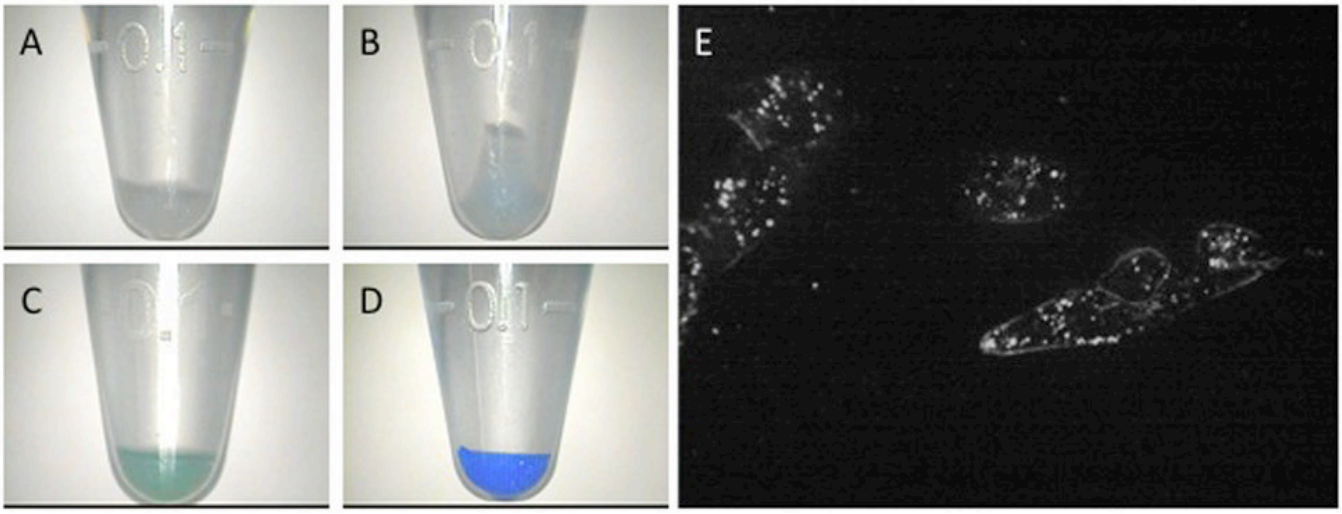

Figure 2.

Visible and microscopic tagging of glioma cell pellets by dye-loaded NPs. Cell samples shown have been treated with 1 mg/mL blank NPs (A), methylene blue-loaded NPs (B), indocyanine green-loaded NPs (C), or CB-loaded NPs (D). Duration of treatment is 15 min for samples C and D and 6 h for A and B. Confocal microscopic images of cells treated with 0.0625 mg F3-targeted methylene blue/CB-loaded NPs for 15 min (E).

NIH-PA Author Manuscript
NIH-PA Author Manuscript
NIH-PA Author Manuscript

NIH-PA Author Manuscript
NIH-PA Author Manuscript
NIH-PA Author Manuscript

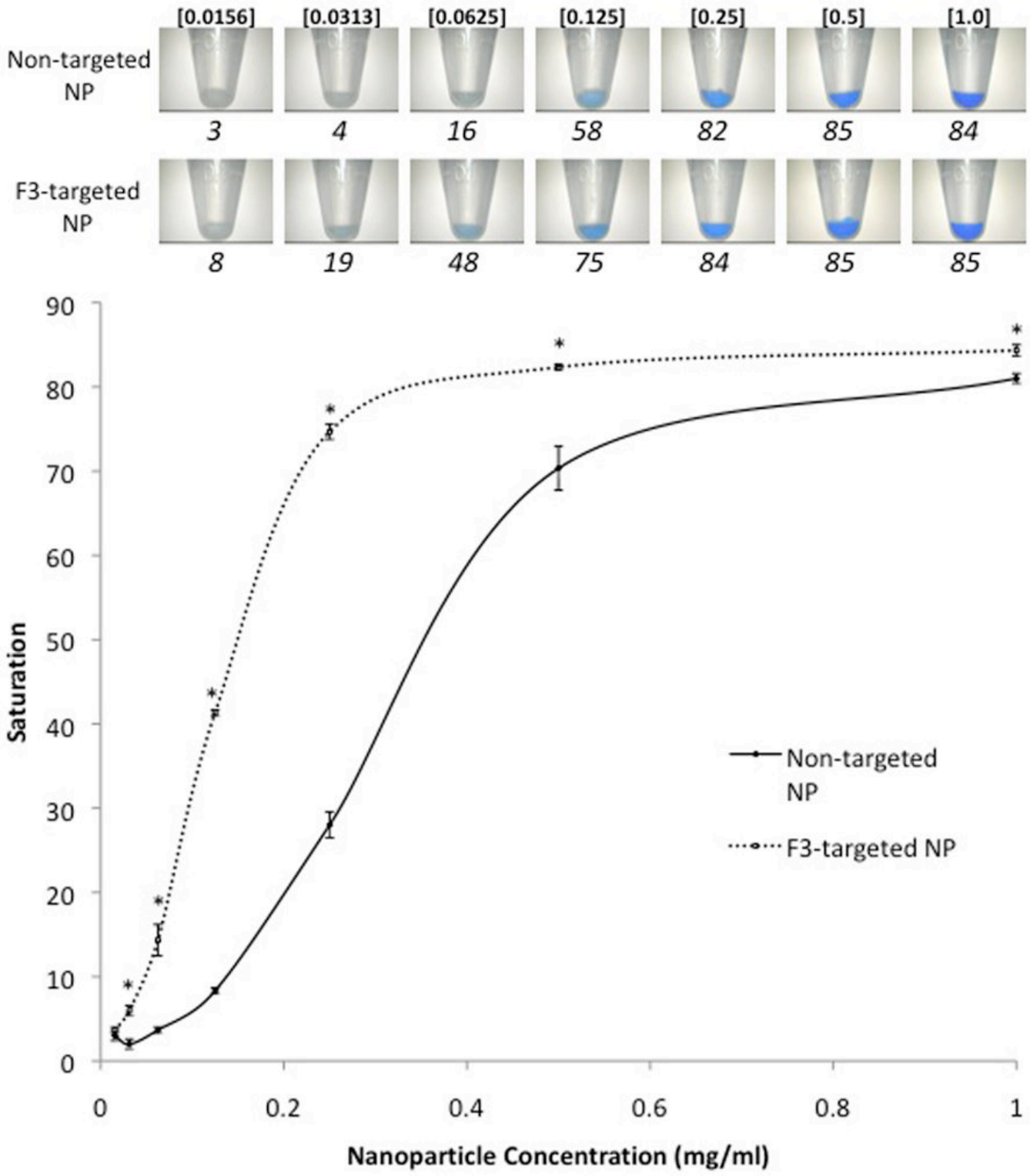

Figure 3. Effect of CB-loaded NP dose on gliosarcoma cell tagging

3A) Images of washed, pelleted 9L gliosarcoma cells after 15 min incubation with increasing doses (shown in *italics*; mg NP/mL) of non-targeted (top) and F3-targeted (bottom) NPs. Note

NIH-PA Author Manuscript

NIH-PA Author Manuscript

NIH-PA Author Manuscript

difference in threshold of blue color visualization in non-targeted and F3-targeted NP-treated cells. Untreated controls (not shown) appear similar to samples treated with 0.0156 mg NP/mL. Corresponding quantified saturation of each cell pellet shown below each sample. 3B) Quantification of blue color saturation in NP-treated cells shown in 3a. Significant differences ($P < 0.01$) between samples at individual doses are indicated by an asterisk (*). Error bars indicate standard error of mean. Saturation values are absolute values and therefore do not have units.

NIH-PA Author Manuscript
NIH-PA Author Manuscript
NIH-PA Author Manuscript

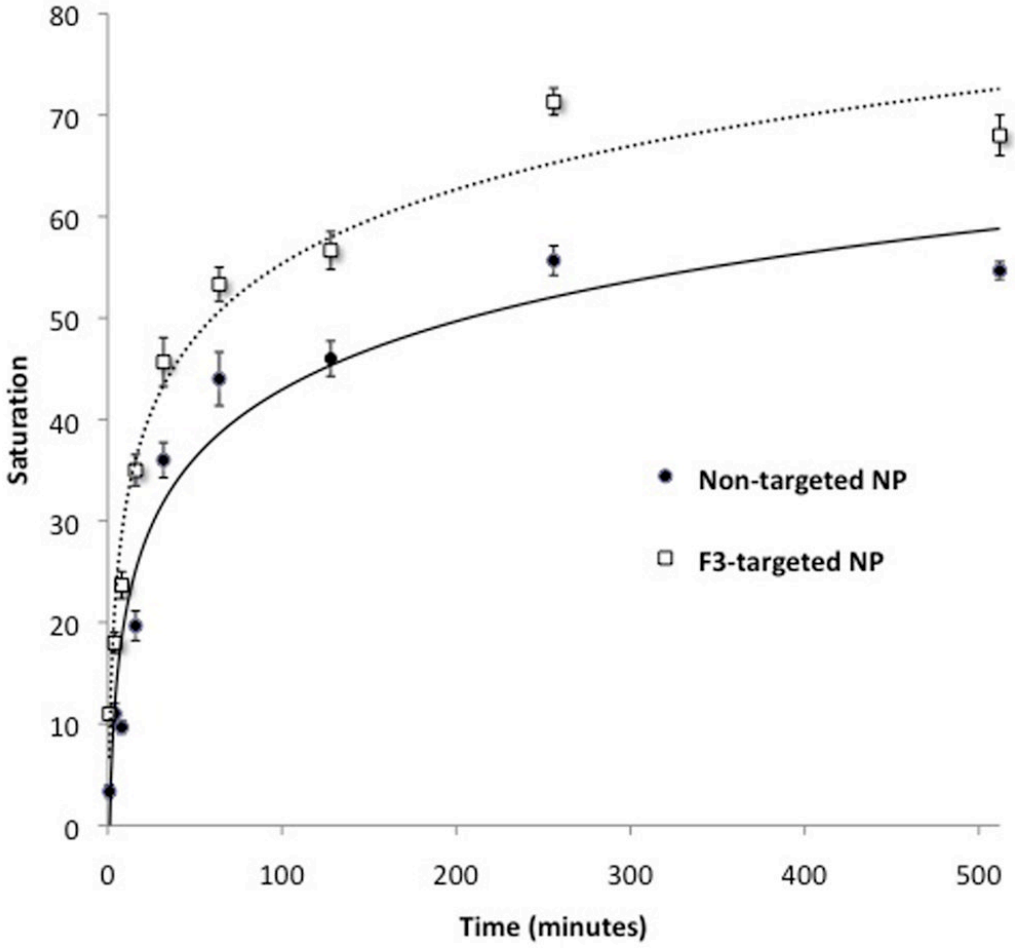

Figure 4.

Effect of treatment duration on gliosarcoma cell tagging by CB-loaded NPs. 9L cells were incubated for varying duration with non-targeted or F3-targeted CB-loaded NPs at time points shown. The extent of tagging is significantly greater for F3-targeted compared to non-targeted NP at all time points ($P < 0.04$). Lines represent best-fit logarithmic curves for non-targeted (R^2=0.94) and F3-targeted (R^2=0.97) NP treatments. Error bars indicate standard error of mean.

NIH-PA Author Manuscript
NIH-PA Author Manuscript
NIH-PA Author Manuscript

A

Cell Line	Nucleolin Expression
MCF-7	1
MDA-435	10.7
9L	6.1

B

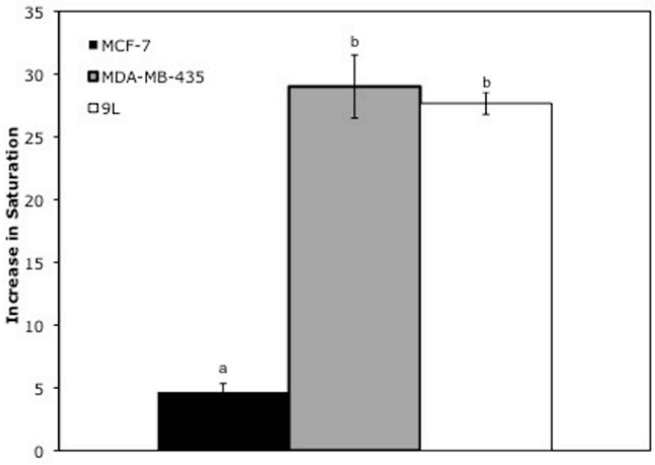

Figure 5.

5A) Relative nucleolin expression: Nucleolin expression was estimated based on uptake of fluorescent F3 peptide by each cell line. All values shown are average fold-increase of uptake of fluorescent peptide by MCF-7 cells. Values shown for MDA-435, and 9L represent a significant increase in fluorescence compared to MCF-7 cells.

5B) Relative increase in glioma cell saturation after treatment with targeted vs. non-targeted NPs: Significant differences ($P < 0.005$), based on unpaired *t*-tests, comparing MCF-7, 9L, and MDA-MB-435 cells are indicated by letters above each data point. Points with statistically significant differences have different letters, while those that are statistically identical share a letter. Error bars indicate standard error of mean.

NIH-PA Author Manuscript

NIH-PA Author Manuscript

NIH-PA Author Manuscript

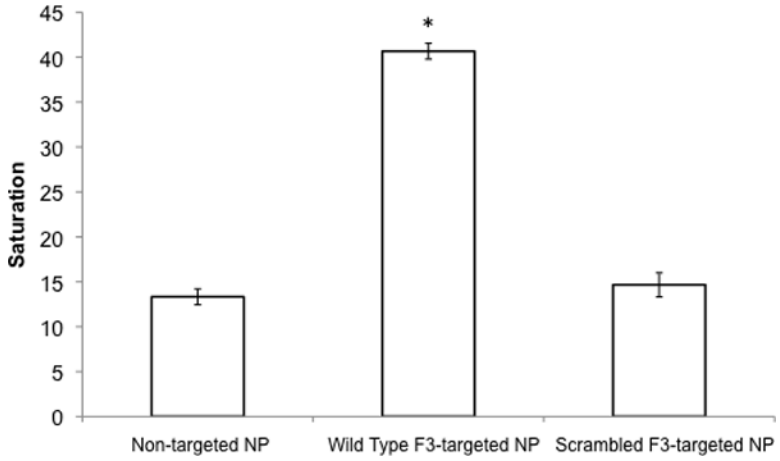

Figure 6.

Comparison of 9L cell uptake for non-targeted, wild-type F3-targeted, and scrambled F3-targeted NPs. Asterisk (*) indicates a significant increase in color change compared to non-targeted NPs. Error bars indicate standard error of mean.